Tutor

Dr. Joaquín F. Pérez de Benito
Departament de Química Física

Grau de Química

Treball Final de Grau

A kinetic study of the permanganate oxidation of L-phenylalanine
Estudi cinètic de l'oxidació permangànica de la L-fenilalanina

Jordi Ferrando Benítez

June 2014

Universitat de Barcelona

Campus d'Excel·lència Internacional
B:KC Barcelona Knowledge Campus

We have a method, and that method helps us to reach not absolute truth, only asymptotic approaches to the truth – never there, just closer and closer, always finding vast new oceans of undiscovered possibilities.

Carl Sagan

Primer de tot m'agradaria agrair al Dr. Joaquín F. Pérez de Benito per tota la paciència que ha tingut durant tots aquests mesos. Ha sigut un tutor excel·lent, del qui he après moltes coses i al qual li desitjo el millor.

També agrair als meus pares per tots els valors i tota l'educació rebuda, sempre estant al meu costat i donant-me bons consells.

Finalment a la Bea, possiblement la persona més sacrificada en tots aquests anys.

REPORT

CONTENTS

1. SUMMARY

The reduction of permanganate ion to $MnO_2 - Mn_2O_3$ soluble colloidal mixed oxide by L-phenylalanine in aqueous phosphate-buffered neutral solutions has been followed by a spectrophotometric method, monitoring the decay of permanganate ion at 525 nm and the formation of the colloidal oxide at 420 nm. The reaction is autocatalyzed by the manganese product and three rate constants have been required to fit the experimental absorbance-time kinetic data. The reaction shows base catalysis and the values of the activation parameters at different pHs have been determined. A mechanism including both the non-autocatalytic and the autocatalytic reaction pathways, and in agreement with the available experimental data, has been proposed. Some key features of this mechanism are the following: (i) of the two predominant forms of the amino acid, the anionic form exhibits a stronger reducing power than the zwitterionic form; (ii) the non-autocatalytic reaction pathway starts with the transfer of the hydrogen atom in the α position of the amino acid to permanganate ion; and (iii) the autocatalytic reaction pathway involves the reduction of Mn(IV) to Mn(II) by the amino acid and the posterior re-oxidation of Mn(II) to Mn(IV) by permanganate ion.

Keywords: autocatalysis, kinetics, mechanism, permanganate ion, L-phenylalanine.

2. RESUM

La reducció de l'ió permanganat a l'òxid col·loïdal soluble mixt $MnO_2 - Mn_2O_3$ per la L-fenilalanina en solució aquosa neutra tamponada amb fosfats s'ha seguit amb un mètode espectrofotomètric, observant la caiguda de l'ió permanganat a 525 nm i la formació de l'òxid col·loïdal a 420 nm. La reacció està autocatalitzada pel producte de manganès i s'han requerit tres constants de velocitat per ajustar les dades cinètiques experimentals d'absorbància-temps. La reacció presenta catàlisi bàsica i s'han determinat els valors dels paràmetres d'activació a diferents pHs. Un mecanisme incloent les vies de reacció no-autocatalítica i autocatalítica ha sigut proposat d'acord amb les dades experimentals obtingudes. Algunes de les característiques clau d'aquest mecanisme són les següents: (i) de les dos formes predominants de l'aminoàcid, la forma aniònica mostra un poder reductor més gran que la forma zwitteriónica; (ii) la via de reacció no-autocatalítica s'inicia amb la transferència de l'àtom d'hidrogen en la posició α de l'aminoàcid a l'ió permanganat; i (iii) la via de reacció autocatalítica implica la reducció de Mn(IV) a Mn(II) per l'aminoàcid i la posterior re-oxidació de Mn(II) a Mn(IV) per l'ió permanganat.

Paraules clau: autocatàlisi, cinètica, mecanisme, ió permanganat, L-fenilalanina.

3. INTRODUCTION

Potassium permanganate is one of the more useful reactants in the chemistry laboratory, and it is widely employed as a versatile oxidizing agent.[1-3] On their part, α-amino acids are important biological compounds, since they are the essential constituents utilized by nature in the synthesis of proteins.[4] Oxidation of α-amino acids is a topic of some interest in relation to cell metabolism. For instance, oxygen free radicals are known to initiate the oxidative degradation of proteins.[5]

The oxidation of α-amino acids by permanganate ion can be used as a simple chemical model for other related reactions of biological importance. As a result, the scientific literature concerning the permanganate-amino acid reactions is abundant. In particular, these redox reactions have been studied in both acidic [6-24] and neutral solutions. [25-39] An important finding of these kinetic studies is the autocatalysis observed in both media.

Autocatalysis is an interesting phenomenon at the theoretical level because of the relatively scarce information existing on this topic. As happens with all catalytic reactions, in the mechanism of autocatalytic processes at least two reaction pathways are involved, one corresponding to the reaction taking place without involvement of the autocatalytic product and the other corresponding to the autocatalytic process, the rate-determining step being different for each reaction pathway. An integrated rate equation that allows the determination of the two rate constants associated to the non-autocatalytic and autocatalytic reaction pathways has been reported.[40-43] However, some deviations from the proposed mathematical model are evident from the experimental kinetic data published for the permanganate-glycine reaction.[44]

In the particular case of the permanganate-amino acid reactions, autocatalysis has been found in both acidic and neutral solutions, in spite of the fact that the manganese reduction product is different in the two media, manganese(II) ion under acidic conditions and colloidal manganese dioxide at near-neutrality pH. As a consequence, doubts have arisen on the identity of the species responsible for the autocatalytic behavior, especially on whether the same autocatalyst is involved in both cases. The present work will focus on the nature of the

autocatalytic agent, and three possibilities [manganese(II), manganese(III) and manganese(IV)] will be considered, checking the consistency of each alternative against the available experimental data.

4. OBJECTIVES

The aim of this investigation is to carry out a kinetic study of the oxidation of L-phenylalanine by permanganate ion in near-neutrality aqueous solutions, in the presence of a KH_2PO_4-K_2HPO_4 buffer. The effect of the latter will be double, to keep the pH of the solution approximately constant as the reaction advances, and to stabilize the manganese oxide particles generated as a reduction product in the form of a soluble colloid. The reaction studied shows an autocatalytic behavior, evidenced by the observation of both sigmoidal concentration against time plots and bell-shaped rate against time plots. The present work will focus on the nature of the autocatalytic agent as well as on the mechanism of the autocatalytic reaction pathway. To that end, experimental determinations of the rate constants corresponding to both the non-autocatalytic and autocatalytic pathways under different reactant mixture conditions will be carried out in a systematic way.

5. EXPERIMENTAL

5.1. MATERIALS AND METHODS

The solvent used in all the experiments was water previously purified by deionization followed by treatment with a Millipore Synergy UV system (milli-Q quality, κ = 0.05 μS/cm at 25.0 ºC). The oxidant was potassium permanganate ($KMnO_4$, Panreac, purity ≥ 99.0%) and the reductant L-phenylalanine (C_6H_5-CH_2-$CH(NH_2)$-COOH, Sigma-Aldrich, purity ≥ 98.0%). The components of the buffer were potassium dihydrogen phosphate (KH_2PO_4, Merck, purity ≥ 99.5%) and potassium hydrogen phosphate trihydrate ($K_2HPO_4 \cdot 3H_20$, Merck, purity ≥ 99.0%).

The pH measurements were done by means of a Metrohm 605 pH-meter, provided with a digital presentation till the third decimal figure (± 0.001 pH) and a combination electrode, calibrated with the aid of two commercial buffers at pH 4.00 ± 0.02 (Merck) and 7.00 ± 0.01 (Sigma-Aldrich). The temperature was kept constant by means of a Julabo thermostatic bath provided with a digital reading (± 0.1 ºC). The spectra were recorded and the absorbances measured with a Shimadzu 160 A UV-Vis spectrophotometer (± 0.001 *A*). The kinetic runs were followed at 5 different wavelengths (350, 420, 467, 525 and 545 nm), measuring the absorbances periodically at time intervals of 30-600 s.

5.2. KINETIC EXPERIMENTS

In most of the experiments the initial concentration of the reducing agent (L-phenylalanine) was much higher than that of the oxidant (permanganate ion) in order to attain an approximately constant concentration of the amino acid (isolation method). In the experiments where the initial concentration of the latter was not large enough, a special program was developed to take into account the decrease of its concentration as the reaction progressed based on the permanganate/amino acid stoichiometric ratio.

The kinetic runs were monitored at 5 wavelengths chosen in the following manner: two corresponding to the twin peaks of the electronic visible spectrum of permanganate ion (525 and 545 nm), one corresponding to the reaction isosbestic point (467 nm), one at the wavelength where permanganate ion is almost transparent (420 nm) and the last at the limit between the UV and Vis regions of the spectrum (350 nm). The most important absorbances to obtain the experimental kinetic data were those corresponding to 420 and 525 nm, the first one allowed monitoring the formation of the manganese reaction product and the other allowed following the decay of permanganate ion.

5.3. KINETIC CALCULATIONS

Two programs were written in BASIC language, one for the determination of two rate constants (k_1 and k_2), and the other for the determination of three rate constants (k_1, k_2 and k_3). In the first program k_1 and k_2 correspond to the non-autocatalytic and autocatalytic reaction pathways, respectively. In the second program k_1 is associated to the non-autocatalytic pathway, whereas both k_2 and k_3 are associated to the autocatalytic one, allowing the

introduction into the mathematical model of a long-lived, non in steady-state intermediate. The calculations were implemented on a Sony Vaio personal computer.

6. SPECTROPHOTOMETRIC BEHAVIOR OF PERMANGANATE ION

The visible spectrum of aqueous permanganate ion has been recorded (Figure 1).

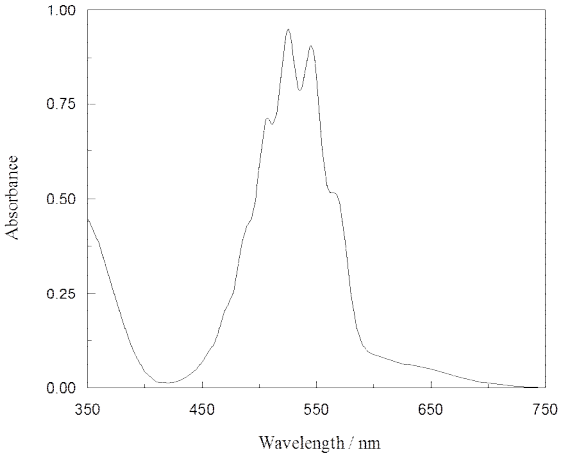

Figure 1. Visible spectrum (350-750 nm) of $KMnO_4$ (4.00×10^{-4} M) in aqueous solution at 25.0 ºC.

This spectrum shows six absorption bands corresponding to different electronic transitions, although two of them are just slightly noticeable shoulders. The highest peak is located at 525 nm with a slightly weaker twin peak at 545 nm. The first wavelength has been selected to follow the disappearance of the oxidant during the reaction. It can also be observed that permanganate is almost transparent to radiation at 420 nm, what explains the violet color of its

aqueous solutions, since all the other visible photons (from red to blue) are efficiently absorbed by the solute. This circumstance has proved to be useful to monitor the formation of one of the reaction products, the soluble form of colloidal manganese dioxide.

Parting from three different permanganate stock solutions, an almost perfect Lambert-Beer behavior has been experimentally found (Figure 2).

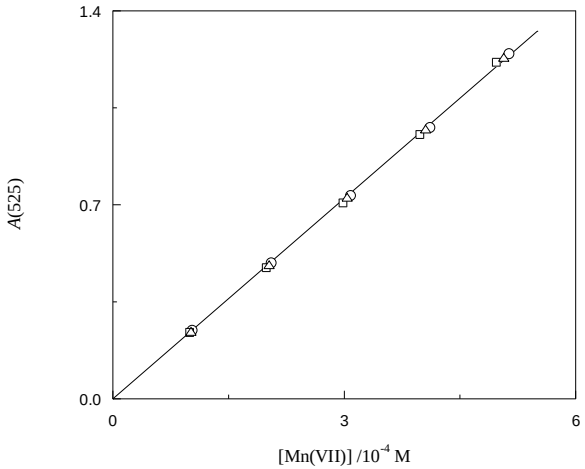

Figure 2. Absorbance at 525 nm as a function of the concentration of permanganate ion in aqueous solution at 25.0 ºC for three independent determinations corresponding to different permanganate stock solutions. (r = 0.99986).

From the slope of that linear plot the value of the molar absorption coefficient of permanganate (limiting reactant of the following kinetic study) at 525 nm is $\varepsilon_{R,525}$ = 2420 ± 10 M^{-1} cm^{-1}.

7. IDENTIFICATION OF THE MANGANESE REDUCTION PRODUCT

The visible spectrum of the manganese reduction product corresponding to a typical kinetic run has been recorded (Figure 3).

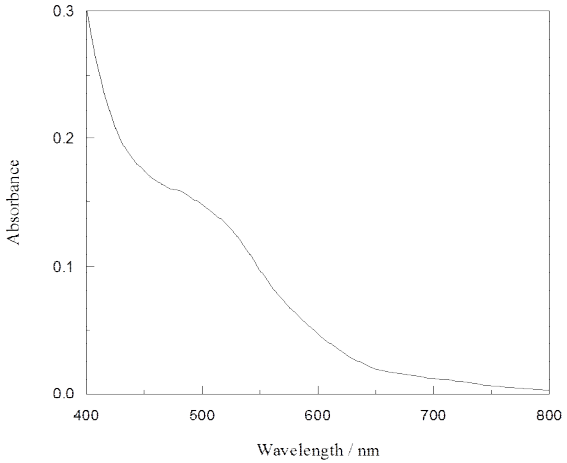

Figure 3. Visible spectrum (400-800 nm) of the manganese reduction product obtained at the end of the reaction. $[KMnO_4]_0 = 4.00 \times 10^{-4}$ M, [L-phenylalanine] = 5.00×10^{-3} M, $[KH_2PO_4] = 0.120$ M, $[K_2HPO_4] = 0.150$ M, $I = 0.570$ M, pH 6.826 ± 0.004, 25.0 ºC.

This spectrum shows the contributions of two different inorganic species: Mn(III), responsible of the shoulder located approximately at the 500-nm region,[45-49] and Mn(IV), present as a soluble form of colloidal MnO_2, responsible of the wide band covering the whole 400-800 nm range. Therefore, the Mn(III) contribution causes the downward-concave curvature of the spectrum whereas Mn(IV) causes the upward-concave curvature. Actually, the origin of the shapeless band of the visible spectrum of the Mn(IV) species can be found in dispersion of light by the colloidal particles and, so, it is related to Rayleigh's law.[50,51]

The final solution had a pink-brownish color, the pink shade being caused by Mn(III) and the brownish shade by Mn(IV), and it was perfectly transparent when the permanganate-amino acid reaction finalized. The stability of this soluble form of colloidal MnO_2 can be attributed to the

binding of phosphate ions (coming from the buffer used in the experiments) to the surface of the colloidal particles.[52] The electrostatic repulsion between them caused by the resulting negative charge slows down the coagulation process. Actually, the activation energy associated to that process increases dramatically as the phosphate concentration increases.[53]

At high concentrations of L-phenylalanine a notable change in the spectrum was observed after all the permanganate ion was totally consumed, so that a definite peak at 462 nm corresponding to Mn(III) could be detected an hour later (Figure 4). The decrease of the absorbance at low wavelengths with time indicates that Mn(IV) was reduced by the amino acid.

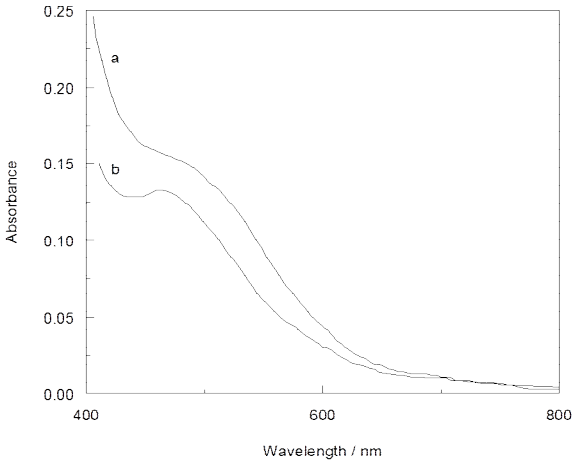

Figure 4. Visible spectra (400-800 nm) of the manganese reduction product recorded at 62 (a) and 134 (b) min after the beginning of the reaction. $[KMnO_4]_0 = 4.00 \times 10^{-4}$ M, [L-phenylalanine] = 5.00×10^{-2} M, $[KH_2PO_4] = 0.120$ M, $[K_2HPO_4] = 0.150$ M, $I = 0.570$ M, pH 6.826 ± 0.004, 25.0 ºC.

The visible spectrum of the manganese reduction product was recorded at different days during the week following the beginning of the reaction (Figure 5). It can be observed that a slight change in the spectrum took place from one day to another, the absorbances at low wavelengths decreasing with time and those at high wavelengths increasing. Simultaneously, the shoulder corresponding to absorption by Mn(III) adopted a more definite profile, indicating that the Mn(III)/Mn(IV) ratio increased.

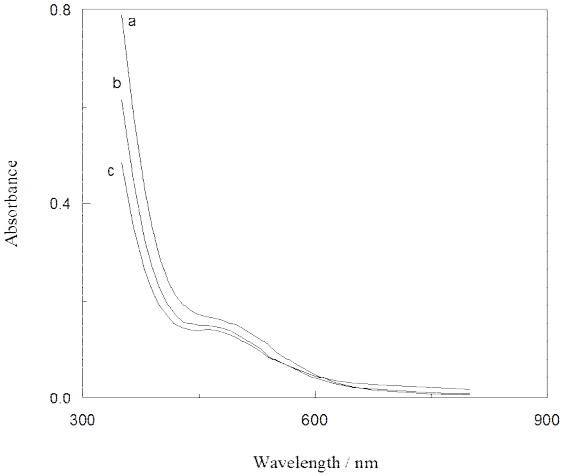

Figure 5. Visible spectra (350-800 nm) of the manganese reduction product recorded 1 (a), 3 (b) and 7 (c) days after the end of the reaction. $[KMnO_4]_0 = 4.00 \times 10^{-4}$ M, [L-phenylalanine] = 5.00×10^{-3} M, $[KH_2PO_4] = 9.60 \times 10^{-2}$ M, $[K_2HPO_4] = 0.180$ M, $I = 0.636$ M, pH 7.02, 20.0 ºC.

Thus, the decrease of absorbance at low wavelengths can be ascribed to the reduction of the Mn(IV) species by the amino acid, whereas the increase at high wavelengths can be ascribed to flocculation of the colloidal particles.

The time required for precipitation to occur depended on the experimental conditions. When the total phosphate concentration ($[KH_2PO_4] + [K_2HPO_4]$) was 0.270 M and the concentration of L-phenylalanine was 5.00×10^{-2} M precipitation occurred one day after the beginning of the reaction, whereas for $[KH_2PO_4] + [K_2HPO_4] = 0.270$ M and [L-phenylalanine] = 5.00×10^{-3} M precipitation occurred after six days. In fact, the precipitation took place gradually, since when it started (as a thin brown powder) most of the colloid still remained in solution. This suggests that the soluble manganese product was present in a distribution of different particle sizes, the bigger ones being the first that precipitated.

In principle, there are two possible alternatives for the nature of the detected Mn(III) species. Given that in slightly acidic or neutral solutions manganese(III) ion, Mn^{3+}, or its hydroxo

complexes, $[Mn(OH)_x]^{(3-x)+}$, would dismutate very rapidly,[54] the only reasonable possibilities would be either a Mn(III)-amino acid complex in the solution or Mn(III) oxide, Mn_2O_3, on the surface of the colloidal particles. However, the notable stability observed in the experiments for the Mn(III) species (Figure 5) suggests that the Mn_2O_3 alternative explanation should be favored over the other one. Effectively, since the amino acid ligand in the complex would be a reducing agent and the metal ion an oxidizing agent, the proposed complex would be expected to behave as an instable species, rather as the Mn(III)-oxalate complex, $[Mn(C_2O_4)]^+$, whose redox decomposition is well known.[55-59] Hence, the manganese reduction product can be regarded as an MnO_2-Mn_2O_3 mixed oxide of soluble colloidal nature.

8. ABSORBANCE PLOTS FOR THE REACTION

All the kinetics runs have been followed at five different wavelengths, 525 and 420 nm being among them. Whereas at the first wavelength both the limiting reactant, permanganate ion, and its reduction product, a soluble form of colloidal manganese oxides (MnO_2-Mn_2O_3), absorb light, the molar absorption coefficient of the reactant being higher than that of the product, at the second wavelength only the product contributes in an appreciable way to the total absorbance.

The absorbance-time experimental data at 420 and 525 nm corresponding to a typical kinetic run appear listed in Appendix 1. This reaction was followed for more than seven hours, corresponding to almost 90% of permanganate reduction.

The absorbances at 420 and 525 nm have been plotted against time for a representative kinetic experiment (Figure 6). A sigmoidal profile can be observed in both *A*(420) vs. *t* and *A*(525) vs. *t* plots, indicating the existence of an autocatalytic phenomenon. At the wavelength corresponding to the formation of the manganese product (420 nm) the plot shows an upward-concave curvature for low reaction times (the reaction rate increases) followed by a downward-concave stretch (the reaction rate decreases), whereas at the wavelength where the decay of permanganate ion predominates (525 nm) is all the way around, the plot showing first a downward-concave curvature (corresponding to the acceleration period) and then an upward-

concave one (corresponding to the slowing-down period). In both cases the inflexion point indicates the instant at which the reaction rate presents a maximum value.

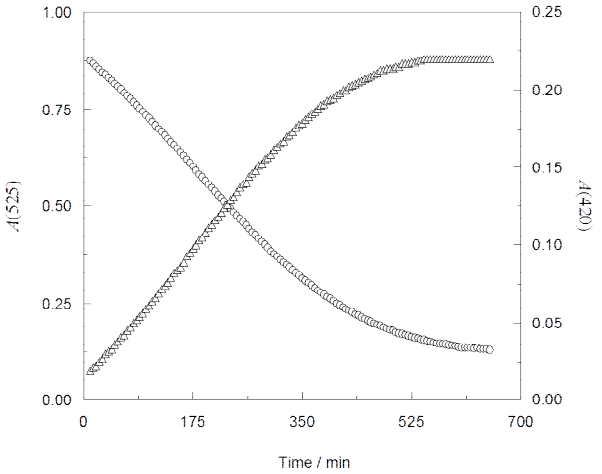

Figure 6. Absorbances at 525 (circles) and 420 (triangles) nm as a function of time during the course of the reaction. $[KMnO_4]_0 = 4.00 \times 10^{-4}$ M, [L-phenylalanine] = 5.00×10^{-3} M, $[KH_2PO_4] = 0.120$ M, $[K_2HPO_4] = 0.150$ M, $I = 0.570$ M, pH 6.826 ± 0.004, 25.0 ºC.

On the other hand, the *A*(467) vs. *t* and *A*(525) vs. *t* plots can be compared in Figure 7.

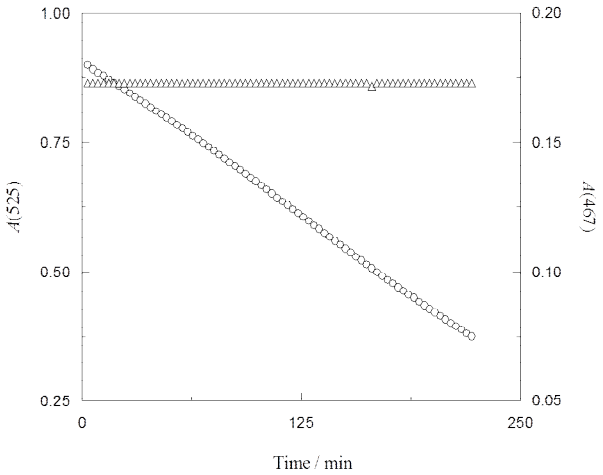

Figure 7. Absorbances at 525 (circles) and 467 (triangles) nm as a function of time during the course of the reaction. $[KMnO_4]_0 = 4.00 \times 10^{-4}$ M, [L-phenylalanine] = 5.00×10^{-3} M, $[KH_2PO_4] = 9.60 \times 10^{-2}$ M, $[K_2HPO_4]$ = 0.180 M, *I* = 0.636 M, pH 7.021 ± 0.004 , 25.0 ºC.

Whereas the absorbance at 525 nm decreased as the reaction proceeded because of the decay of the limiting reactant (permanganate ion) concentration, that at 467 nm was constant, indicating the existence of an isosbestic point at the latter wavelength. It can then be concluded that the molar absorption coefficients of permanganate ion and the manganese reduction product at 467 nm are equal ($\varepsilon_{R,467} = \varepsilon_{P,467}$).[60a]

Additionally, the experimental values of the absorbance at 525 nm have been represented against those of the absorbance at 420 nm in Figure 8.

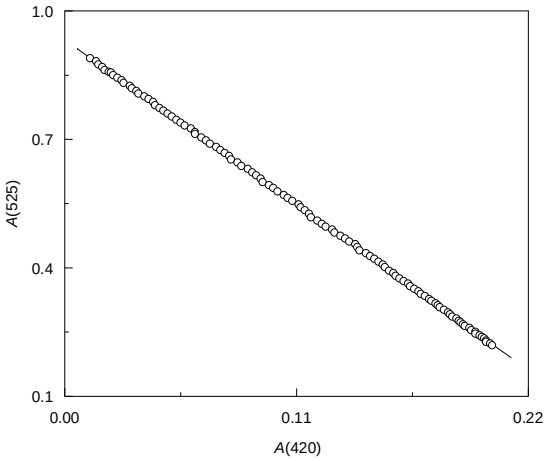

Figure 8. Absorbance at 525 nm as a function of the absorbance at 420 nm (r = 0.99996) from experimental measurements at 4-min intervals. $[KMnO_4]_0 = 4.00 \times 10^{-4}$ M, [L-phenylalanine] = 5.00×10^{-3} M, $[KH_2PO_4]$ = 0.120 M, $[K_2HPO_4]$ = 0.150 M, I = 0.570 M, pH 6.826 ± 0.004, 25.0 ºC.

It can be seen in that figure that, during the course of the reaction, the absorbance at 525 nm decreases in a linear way as the absorbance at 420 nm increases. This kind of behavior can be easily explained from the following mathematical considerations. Let us start writing the total absorbances at 420 and 525 nm as a sum of the independent contributions of the reactant, permanganate ion (R), and the product, a colloidal combined MnO_2-Mn_2O_3 manganese oxide (P):

$$A(420) = A(420)_R + A(420)_P \quad (1)$$

$$A(525) = A(525)_R + A(525)_P \quad (2)$$

Assuming now that the two species fulfill the Lambert-Beer law at both wavelengths:

$$A(420)_R = \varepsilon_{R,420}\, l\, [MnO_4^-] \quad (3)$$

$$A(525)_R = \varepsilon_{R,525}\, l\, [MnO_4^-] \quad (4)$$

$$A(420)_P = \varepsilon_{P,420}\, l\, [MnO_2] \quad (5)$$

$$A(525)_P = \varepsilon_{P,525}\, l\, [MnO_2] \quad (6)$$

where the subscripts of the molar absorption coefficients indicate the corresponding species (R or P) and wavelengths, whereas l is the optical path length (1 cm). Replacing these results into eqs 1 and 2, the total absorbances at 420 and 525 nm can be expressed as:

$$A(420) = \varepsilon_{R,420}\, l\, [MnO_4^-] + \varepsilon_{P,420}\, l\, [MnO_2] \quad (7)$$

$$A(525) = \varepsilon_{R,525}\, l\, [MnO_4^-] + \varepsilon_{P,525}\, l\, [MnO_2] \quad (8)$$

Since permanganate ion is almost transparent to the radiation at 420 nm, its contribution to the total absorbance at that wavelength can be neglected ($\varepsilon_{R,420} \approx 0$). Thus, from eq 7 it can be approximated that:

$$A(420) = \varepsilon_{P,420}\, l\, [MnO_2] \quad (9)$$

On the other hand, the principle of mass conservation allows writing:

$$[MnO_4^-]_o = [MnO_4^-] + [MnO_2] \quad (10)$$

where it has been considered that the total manganese concentration is constant during the kinetics runs, as well as that the concentrations of the manganese intermediates involved in the

reaction mechanism are negligible. That approximation is indeed reasonable provided that the mentioned intermediates are in steady state. This hypothesis can be applied only to intermediates very dilute with respect to the limiting reactant, although not necessarily in almost constant concentration, contrarily to what is usually understood.[60b]

In order to simplify the notation, let us symbolize the permanganate concentration at time *t* during the course of the reaction by *c* and its initial value by c_o. Then, eqs 8-10 become:

$$A(525) = \varepsilon_{R,525}\, l\, c + \varepsilon_{P,525}\, l\, (c_o - c) \tag{11}$$

$$A(420) = \varepsilon_{P,420}\, l\, (c_o - c) \tag{12}$$

From eq 12, it can be obtained the permanganate concentration at time *t*:

$$c = c_o - \frac{A(420)}{\varepsilon_{P,420}\, l} \tag{13}$$

and that of colloidal manganese dioxide at the same instant:

$$c_o - c = \frac{A(420)}{\varepsilon_{P,420}\, l} \tag{14}$$

From eqs 11, 13 and 14:

$$A(525) = \varepsilon_{R,525}\, l\, c_o - \left(\frac{\varepsilon_{R,525} - \varepsilon_{P,525}}{\varepsilon_{P,420}}\right) A(420) \tag{15}$$

and given that the Lambert-Beer law allows to express the initial absorbance at 525 nm as:

$$A(525)_o = \varepsilon_{R,525}\, l\, c_o \tag{16}$$

from eqs 15 and 16 it can be finally obtained:

$$A(525) = A(525)_o - \left(\frac{\varepsilon_{R,525} - \varepsilon_{P,525}}{\varepsilon_{P,420}} \right) A(420) \quad (17)$$

Equation 17 predicts that an *A*(525) vs *A*(420) plot would be linear provided that the molar absorption coefficients of the colloidal manganese dioxide species at both 420 and 525 nm are approximately constant during the course of the reaction. Since the experimental results shown in Figure 8 confirm that the plot is actually linear, it can be concluded the validity of this hypothesis. This means that the soluble form of MnO_2 generated as a reaction product behaves as a rather stable species, the size of its colloidal particles remaining constant during the kinetics run. Moreover, the linearity of that plot confirms also the hypothesis that all the possible manganese intermediates are in steady state (see eq 10).

Actually, *A*(525)–*A*(420) plots similar to that shown in Figure 8 have been reported in the permanganate-related chemical literature, yielding useful information on the behavior of the colloidal MnO_2 species formed in the reactions.[61-63]

9. REDUCTION OF COLLOIDAL MANGANESE DIOXIDE

Since permanganate ion is almost transparent to radiation at 420 nm, this wavelength is useful to monitor the evolution of the concentration of the manganese reaction products with time. When a high L-phenylalanine concentration was present in the solution, two well-definite steps could be observed in the absorbance-time plots (Figure 9). In the first step the absorbance increased as a result of the formation of colloidal MnO_2-Mn_2O_3, whereas in the second step the absorbance decreased due to the reduction of MnO_2 by the amino acid.

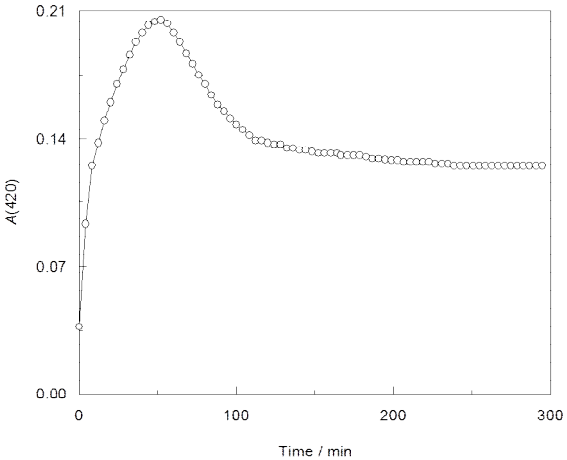

Figure 9. Absorbance at 420 nm as a function of time from experimental measurements at 4-min intervals. $[KMnO_4]_0 = 4.00 \times 10^{-4}$ M, [L-phenylalanine] = 5.00×10^{-2} M, $[KH_2PO_4] = 0.120$ M, $[K_2HPO_4] = 0.150$ M, $I = 0.570$ M, pH 6.826 ± 0.004, 25.0 ºC.

An estimation of the rate of reduction of colloidal MnO_2 by the organic substrate was possible because a stretch of the second step corresponding to the decrease of the absorbance at 420 nm could be fitted to a pseudo-first order plot (Figure 10). The value of the pseudo-first order rate constant so obtained was $k = (5.29 \pm 0.10) \times 10^{-4}$ s^{-1}.

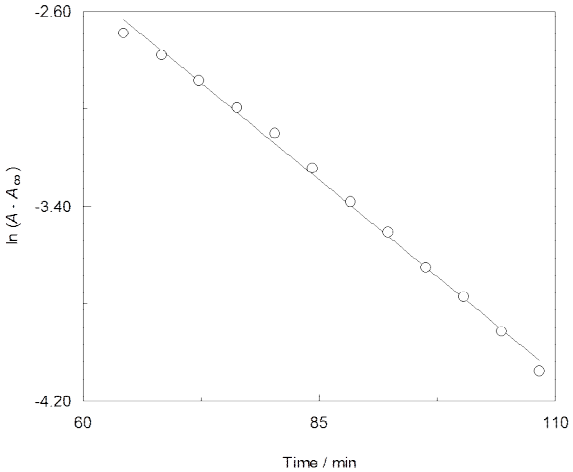

Figure 10. Pseudo-first order plot for the absorbance at 420 nm after complete reduction of permanganate ion. $[KMnO_4]_o = 4.00 \times 10^{-4}$ M, [L-phenylalanine] = 5.00×10^{-2} M, $[KH_2PO_4] = 0.120$ M, $[K_2HPO_4] = 0.150$ M, $I = 0.570$ M, pH 6.826 ± 0.004, 25.0 ºC.

10. FROM THE EXPERIMENTAL ABSORBANCE-TIME DATA TO THE REACTION RATE

In order to calculate the concentration of the limiting reactant (permanganate ion) at different instants during the course of the reaction from the experimental absorbance-time data, eq 2 can be rewritten to obtain the contribution of that reactant to the total absorbance measured at 525 nm as:

$$A(525)_R = A(525) - A(525)_P \quad (18)$$

Application of the Lambert-Beer law to the light-absorbing reaction product (colloidal MnO_2) at both 420 and 525 nm (eqs 5 and 6) leads to:

$$A(525)_P = \frac{\varepsilon_{P,525}}{\varepsilon_{P,420}} A(420) \quad (19)$$

where it has been considered that at 420 nm only the product contributes in an appreciable way to the experimental absorbance. From eqs 18 and 19:

$$A(525)_R = A(525) - \frac{\varepsilon_{P,525}}{\varepsilon_{P,420}} A(420) \quad (20)$$

Since at $t = \infty$ the limiting reactant (permanganate ion) has been totally reduced by the amino acid, the species absorbing light at both wavelengths is the colloid. Thus, from eqs 5 and 6:

$$\frac{\varepsilon_{P,525}}{\varepsilon_{P,420}} = \frac{A(525)_\infty}{A(420)_\infty} \quad (21)$$

and from eqs 20 and 21:

$$A(525)_R = A(525) - \frac{A(525)_\infty}{A(420)_\infty} A(420) \quad (22)$$

whereas application of the Lambert-Beer law to the oxidant (eq 4) yields:

$$[MnO_4^-] = \frac{1}{\varepsilon_{R,525}\, l} \left[A(525) - \frac{A(525)_\infty}{A(420)_\infty} A(420)\right] \quad (23)$$

Equation 23 can be used to obtain the values of the permanganate concentration at several instants during the course of the reaction from the corresponding experimental absorbances at 420 and 525 nm.

The values of the reaction rate have been obtained from those of the permanganate concentration by means of the finite difference method. This mathematical procedure of

approximate derivation allows the calculation of the rate at time $t + \Delta t/2$ from the permanganate concentrations at times t and $t + \Delta t$ as:

$$v = -\frac{\mathrm{d}[\mathrm{MnO_4^-}]}{\mathrm{d}t} \approx \frac{c(t) - c(t+\Delta t)}{\Delta t} \quad (24)$$

Since the permanganate concentration decreases during the reaction, that is $c(t) > c(t+\Delta t)$, the rate given by eq 24 is already in absolute value. This approximate method allows calculating the reaction rate with a very low systematic error provided that the time interval chosen (Δt) is small enough.

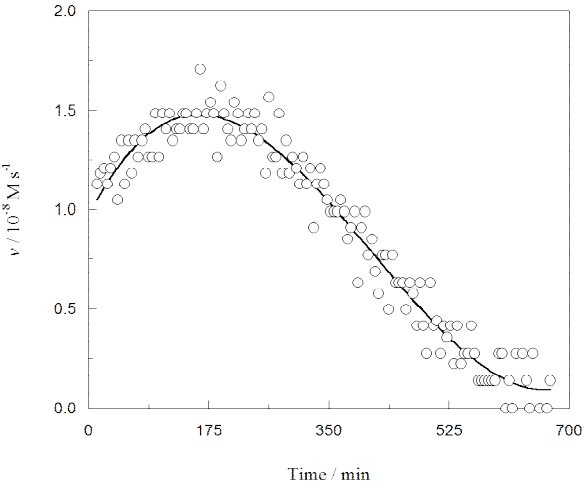

Figure 11. Reaction rate as a function of time from experimental measurements at 5-min intervals. $[KMnO_4]_0 = 4.00 \times 10^{-4}$ M, [L-phenylalanine] = 5.00×10^{-3} M, $[KH_2PO_4] = 0.120$ M, $[K_2HPO_4] = 0.150$ M, $I = 0.570$ M, pH 6.826 ± 0.004, 25.0 ºC.

The reaction rate has been plotted against time for a typical kinetic run in Figure 11. The values of the permanganate concentration were obtained by application of eq 23 and those of the rate by application of eq 24.

It can be seen in Figure 11 that the curve shows a definite bell-shape pattern, since the rate increases from the beginning of the reaction, reaches a maximum and then decreases, thus confirming that the process is in fact autocatalytic, the maximum seen in Figure 11 corresponding to the inflexion points in the absorbance vs. time curves of Figure 6.

11. TWO RATE-CONSTANT KINETIC MODEL FOR AUTOCATALYSIS

The total reaction rate for an autocatalytic reaction can be expressed as a sum of the independent contributions of the non-autocatalytic (v_1) and the autocatalytic (v_2) pathways:

$$v = v_1 + v_2 \tag{25}$$

The simplest form of the differential rate law for an autocatalytic reaction assumes that both reaction pathways are of first order in the limiting reactant (in our case, permanganate ion) and that the autocatalytic pathway is also of first order in the autocatalyst (colloidal manganese dioxide). Hence:

$$v = k_1 [\mathrm{MnO_4^-}] + k_2 [\mathrm{MnO_4^-}] [\mathrm{MnO_2}] \tag{26}$$

Now, assuming again that all the manganese intermediates are in negligible concentration with respect to Mn(VII) and Mn(IV), that is in steady state, eq 26 can be rewritten as:

$$v = k_1 c + k_2 c (c_o - c) \tag{27}$$

or in a linearized way:

$$\frac{v}{c} = (k_1 + k_2\, c_o) - k_2\, c \qquad (28)$$

Equation 27 has been reported to be useful for the kinetic study of the permanganate oxidation of aliphatic amines in aqueous phosphate buffers.[64-68]

On the other hand, it can be seen that eq 28 predicts a linear plot when the rate-permanganate concentration ratio is plotted against the permanganate concentration at different instants during the course of the reaction. A typical example can be seen in Figure 12 for the kinetic run corresponding to the absorbance-time experimental data listed in Appendix 1.

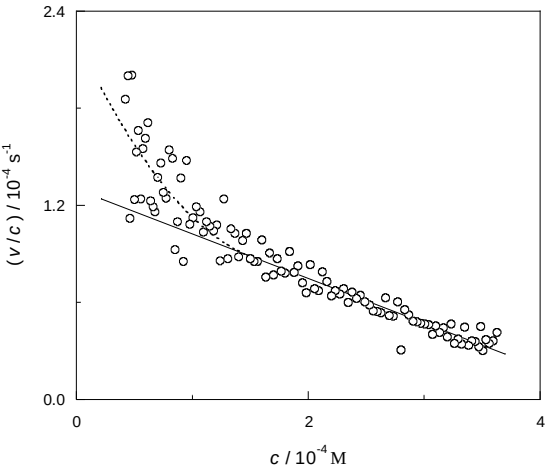

Figure 12. Reaction rate-permanganate concentration ratio as a function of the concentration of permanganate ion calculated at periodical 4-min intervals during the course of a typical kinetic run (the direction of the reaction progress is from right to left). $[KMnO_4]_o = 4.00 \times 10^{-4}$ M, [L-phenylalanine] = 5.00×10^{-3} M, $[KH_2PO_4] = 0.120$ M, $[K_2HPO_4] = 0.150$ M, $I = 0.570$ M, pH 6.826 ± 0.004, 25.0 ºC.

For a pseudo-first order kinetics the *v*/*c* ratio would be expected to remain constant as the reaction progresses. However, an increase of that ratio can be observed in Figure 12, indicating again the existence of an autocatalytic phenomenon. Although the first stretch is approximately linear, a definite upward-concave curvature can be seen at high reaction times.

A simple mathematical treatment (separation of variables followed by integration) allows obtaining from eq 27 the integrated rate law for an autocatalytic reaction:

$$\ln \frac{k_1 + k_2 c_o - k_2 c}{c} = \ln\left(\frac{k_1}{c_o}\right) + (k_1 + k_2 c_o) t \qquad (29)$$

By using an iterative procedure (starting with some trial values of the rate constants) the correct values of k_1 and k_2 can be inferred from eq 29. A graphical representation of the fit of the experimental data to this equation can be seen in Figure 13.

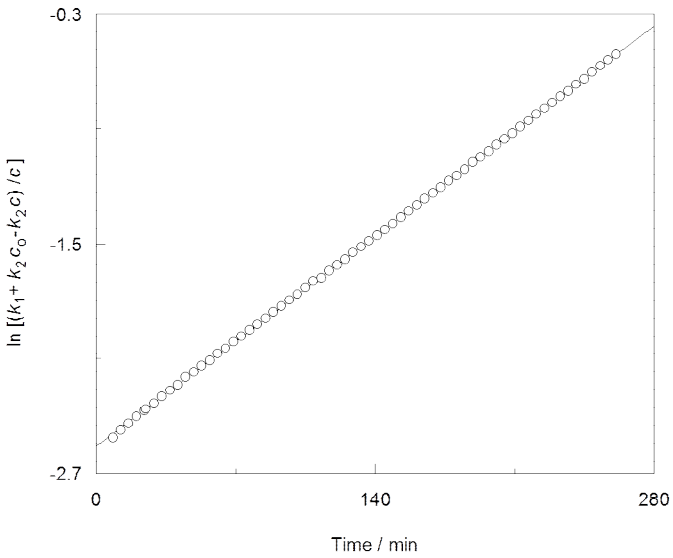

Figure 13. Left-hand side of eq 29 as a function of time. $[KMnO_4]_0 = 4.00 \times 10^{-4}$ M, [L-phenylalanine] = 5.00×10^{-3} M, $[KH_2PO_4] = 0.120$ M, $[K_2HPO_4] = 0.150$ M, $I = 0.570$ M, pH 6.826 ± 0.004, 25.0 ºC.

This iterative mathematical procedure has been repeated for several numbers of experimental points (*N*) and the results are shown in Table 1.

N	% Reaction	k_1 / 10^{-5} s^{-1}	k_2 / $M^{-1}s^{-1}$	*r*	*E* / 10^{-4}
25	21.3	3.02	0.242	0.999952	3.41
35	30.7	3.01	0.244	0.999967	4.37
45	40.5	2.97	0.255	0.999975	5.43
55	50.5	2.89	0.270	0.999972	7.48
65	59.6	2.82	0.282	0.999968	9.14

(a) % Reaction is the percentage of permanganate ion reduced for each *N* value.
(b) *r* is the linear regression coefficient corresponding to eq 29.
(c) *E* is the average error of the theoretical absorbances predicted by eq 29 with respect to the experimental ones.

Table 1. Values of the pseudo-rate constants for the non-autocatalytic (k_1) and the autocatalytic (k_2) reaction pathways as a function of the number of experimental points included in the linear regression. $[KMnO_4]_0 = 4.00 \times 10^{-4}$ M, [L-phenylalanine] = 5.00×10^{-3} M, $[KH_2PO_4] = 0.120$ M, $[K_2HPO_4] = 0.150$ M, $I = 0.570$ M, pH 6.826 ± 0.004, 25.0 ºC.

It can be seen that, although the linear regressions corresponding to the integrated rate law are reasonably good ($r > 0.9999$), the values of the rate constants show a notable dependence on the number of experimental points used in the linear fit, since k_1 decreased and k_2 increased with increasing *N*. Given that the values of the pseudo-rate constants should not change with time, it seems that eqs 27 (differential rate law) and 29 (integrated rate law) are not the best choices to describe the kinetic behavior of the permanganate-phenylalanine reaction, and that a new mathematical model is required.

12. THREE RATE-CONSTANT KINETIC MODEL FOR AUTOCATALYSIS

The apparent increase of the pseudo-rate constant for the autocatalytic reaction pathway (k_2) with time seen in Table 1 suggests that the catalytic power of the colloidal manganese product increases as the reaction advances. This feature can be explained if it is assumed that

Mn(IV) is slowly reduced by the amino acid to Mn(II), so that the [Mn(II)]/[Mn(IV)] ratio increases with time, and that Mn(II) is oxidized by permanganate ion. Moreover, it can also be concluded that the Mn(VII)-Mn(II) reaction is not fast enough for the intermediate Mn(II) to be in steady state. This means that three rate constants instead of two (as in eqs 27 and 29) have to be included in the correct kinetic model, one for the non-autocatalytic pathway (k_1) corresponding to the permanganate-amino acid reaction taking place in the solution to yield MnO_2, and two for the autocatalytic pathway taking place on the surface of the manganese colloidal particles, one of them corresponding to the reduction of MnO_2 by L-phenylalanine to yield MnO (k_2) and the other corresponding to the oxidation of the latter by permanganate ion (k_3).

Given that a three rate-constant integrated kinetic equation for autocatalytic reactions is not available in the chemical literature, and that it cannot be mathematically deduced either because of the involvement of the concentration of an intermediate (MnO) that cannot be expressed as a function of the permanganate concentration as a result of its not being in steady state, it has been necessary the use of a numerical simulation method.

The derivatives of the three relevant manganese concentrations with respect to time can be expressed as:

$$\frac{d[Mn(VII)]}{dt} = -v_1 - v_3 \quad (30)$$

$$\frac{d[Mn(IV)]}{dt} = v_1 - v_2 + 2v_3 \quad (31)$$

$$\frac{d[Mn(II)]}{dt} = v_2 - v_3 \quad (32)$$

where v_1 is the rate of the first step [formation of Mn(IV) from Mn(VII)], v_2 is the rate of the second step [formation of Mn(II) from Mn(IV)] and v_3 is the rate of the third step [oxidation of Mn(II) by Mn(VII) to yield Mn(IV)]. Using the respective rate constants:

$$\frac{d[Mn(VII)]}{dt} = -k_1[Mn(VII)] - k_3[Mn(VII)][Mn(II)] \quad (33)$$

$$\frac{\mathrm{d}[\mathrm{Mn(IV)}]}{\mathrm{d}t} = k_1\,[\mathrm{Mn(VII)}] - k_2\,[\mathrm{Mn(IV)}] + 2\,k_3\,[\mathrm{Mn(VII)}]\,[\mathrm{Mn(II)}] \quad (34)$$

$$\frac{\mathrm{d}[\mathrm{Mn(II)}]}{\mathrm{d}t} = k_2\,[\mathrm{Mn(IV)}] - k_3\,[\mathrm{Mn(VII)}]\,[\mathrm{Mn(II)}] \quad (35)$$

In eqs 33-35 it has been assumed that the concentration of L-phenylalanine is in large excess with respect to that of permanganate ion (isolation method). Although in a few experiments the [reductant]/[oxidant] ratio was not large enough, this circumstance can be easily corrected in the simulations when necessary. It can be checked that eqs 30-35 are consistent with the principle of mass conservation, since the sum of the three derivatives is equal to zero, thus corresponding to a constant value of the total manganese concentration. Although at the end of the kinetic experiments the presence of Mn(III) was clearly detectable in the UV-Vis spectra, in order to simplify the calculations it has been assumed that its concentration is negligible. Even if this condition is not fulfilled, the numerical simulations would be correct provided that the [Mn(III)]/[Mn(IV)] ratio remains approximately constant during the progress of the reaction. Actually, this second condition is consistent with the straight line shown in Figure 8, since the average values of the molar absorption coefficients at 420 and 525 nm for the Mn(III)-Mn(IV) product mixture must be almost constant during the process of the reaction for the linear relationship corresponding to eq 17 to hold.

The numerical simulations chosen for the approximate integration of eqs 33-35 were those corresponding to the fourth-order Runge-Kutta method.[69] This procedure is similar to the finite difference method (eq 24) but in the opposite direction (derived function $\rightarrow$ integrated function). A computer program in BASIC language has been developed allowing the determination of four fitting parameters (the initial absorbance and the three rate constants involved) for each kinetic experiment. Starting with some trial values of those parameters, different combinations were used until the error of the simulation was minimized. This error was defined as:

$$E = \frac{\sum_{\mathrm{i}=1}^{N} \left| A_{\mathrm{i,sim}} - A_{\mathrm{i,exp}} \right|}{N} \quad (36)$$

where $A_{i,sim}$ and $A_{i,exp}$ are the numerically simulated and experimental values of the absorbance at different instants during the course of the reaction, and N is the number of points at which the absorbances were measured for each kinetic run. The simulation method applied yielded an excellent concordance between the theoretical and experimental absorbances provided that the time interval (Δt) used in the calculations for the approximate integration of eqs 33-35 was short enough. Depending on the experimental conditions, Δt spanned from 30 s (fast reactions) to 10 min (slow reactions), and the error value (*E)* from 3.13 $\times$ 10^{-4} to 1.03 $\times$ 10^{-3}.

13. KINETIC RESULTS

13.1. EFFECT OF THE INITIAL OXIDANT CONCENTRATION

A series of kinetic runs was performed at different initial permanganate concentrations, all the other experimental conditions remaining constant. The results are shown in Table 2.

$[KMnO_4]_o$ / 10^{-4} M	k_1 / 10^{-5} s^{-1}	k_2 / 10^{-4} s^{-1}	k_3 / M^{-1} s^{-1}
2.00	4.59 ± 0.21	0.71 ± 0.14	1.289 ± 0.048
4.00	3.31 ± 0.05	3.61 ± 0.12	0.439 ± 0.009
6.00	2.87 ± 0.13	5.37 ± 1.04	0.296 ± 0.011
8.00	2.43 ± 0.04	10.02 ± 1.00	0.218 ± 0.004
10.00	2.22 ± 0.05	10.59 ± 0.27	0.200 ± 0.003

(a) Errors were calculated as a half of the range (2 determinations).

Table 2. Values of the pseudo-rate constants at several initial permanganate concentrations. [L-phenylalanine] = 5.00 $\times$ 10^{-3} M, [KH_2PO_4] = 0.120 M, [K_2HPO_4] = 0.150 M, *I* = 0.570 M, pH 6.826 ± 0.004, 25.0 ºC.

Although it is clear that well-determined pseudo-rate constants should not depend on the initial concentration of the limiting reactant (permanganate ion) species, a certain dependence on that variable can be observed in the three constants. Whereas both k_1 and k_3 decreased with increasing permanganate concentration, k_2 increased. In fact a certain dependence of the rate constants on the initial oxidant concentration has been reported in many kinetic studies of permanganate reactions.[70]

13.2. EFFECT OF THE INITIAL REDUCTANT CONCENTRATION

The rate constant values corresponding to a kinetic series performed at different initial reductant concentrations with all the other experimental conditions kept unchanged are listed in Table 3.

$[\text{L-Phenyalanine}]_o$ / 10^{-3} M	k_1 / 10^{-5} s^{-1}	k_2 / 10^{-4} s^{-1}	k_3 / M^{-1} s^{-1}
2.00	1.66 ± 0.04	2.08 ± 0.27	0.169 ± 0.002
2.50	2.17 ± 0.16	2.31 ± 0.29	0.207 ± 0.001
3.00	2.16 ± 0.10	4.67 ± 0.21	0.231 ± 0.004
3.50	2.56 ± 0.05	3.13 ± 0.35	0.284 ± 0.015
4.00	2.69 ± 0.22	3.14 ± 0.70	0.337 ± 0.014
4.50	3.04 ± 0.30	2.95 ± 0.60	0.385 ± 0.019
5.00	3.31 ± 0.05	3.61 ± 0.12	0.439 ± 0.009
5.50	3.42 ± 0.01	3.54 ± 0.08	0.420 ± 0.009
6.00	3.90 ± 0.14	2.65 ± 0.23	0.506 ± 0.018
6.50	4.02 ± 0.10	2.52 ± 0.05	0.570 ± 0.001
7.00	4.22 ± 0.03	2.86 ± 0.01	0.590 ± 0.013

(a) Errors were calculated as a half of the range (2 determinations).

Table 3. Values of the pseudo-rate constants at several initial L-phenyalanine concentrations. $[KMnO_4]$ = 4.00×10^{-4} M, $[KH_2PO_4]$ = 0.120 M, $[K_2HPO_4]$ = 0.150 M, I = 0.570 M, pH 6.826 ± 0.004, 25.0 ºC.

An increase of both k_1 and k_3 with increasing initial reductant concentration was found, whereas k_2 remained approximately constant.

13.3. EFFECT OF THE IONIC STRENGTH

Table 4 contains the results corresponding to a kinetic series designed to study the effect of the ionic strength of the medium on the reaction rate, using potassium chloride as inert electrolyte.

[KCl] / M	pH	k_1 / 10^{-5} s^{-1}	k_2 / 10^{-4} s^{-1}	k_3 / M^{-1} s^{-1}
0.000	6.826 ± 0.004	3.31 ± 0.05	3.61 ± 0.12	0.439 ± 0.009
0.120	6.786 ± 0.002	3.89 ± 0.12	1.58 ± 0.24	0.586 ± 0.063
0.240	6.745 ± 0.002	4.03 ± 0.01	1.40 ± 0.12	0.522 ± 0.040
0.360	6.718 ± 0.001	4.10 ± 0.06	1.36 ± 0.21	0.510 ± 0.069
0.480	6.689 ± 0.001	4.29 ± 0.04	1.00 ± 0.04	0.535 ± 0.005

(a) Errors were calculated as a half of the range (2 determinations).

Table 4. Values of the pseudo-rate constants at several potassium chloride concentrations. [$KMnO_4$] = 4.00×10^{-4} M, [L-phenylalanine] = 5.00×10^{-3} M, [KH_2PO_4] = 0.120 M, [K_2HPO_4] = 0.150 M, I = 0.570 M + [KCl], 25.0 ºC.

An increase in the potassium chloride concentration resulted in an increase of k_1 and a decrease of k_2, whereas k_3 remained almost constant.

13.4. EFFECT OF THE PH

The influence of the medium pH on the rate constants was studied at five different temperatures, in the range 20.0-40.0 ºC. The results are shown in Tables 5-9. It can be observed that the three rate constants increased with increasing pH at the five temperatures studied (base catalysis).

pH	k_1 / 10^{-5} s^{-1}	k_2 / 10^{-4} s^{-1}	k_3 / M^{-1} s^{-1}
6.655 ± 0.009	1.44 ± 0.01	2.33 ± 0.13	0.125 ± 0.002
6.826 ± 0.004	2.04 ± 0.03	3.13 ± 0.25	0.212 ± 0.014
7.021 ± 0.004	3.04 ± 0.08	3.00 ± 0.02	0.304 ± 0.010
7.229 ± 0.006	3.76 ± 0.03	5.96 ± 0.03	0.342 ± 0.002
7.471 ± 0.007	5.26 ± 0.06	9.44 ± 0.19	0.441 ± 0.002

(a) Errors associated to the pH values are standard deviations (10 determinations).
(b) Errors associated to the pseudo-rate constants were calculated as a half of the range (2 determinations).

Table 5. Values of the pseudo-rate constants at 20.0 ºC and different pHs. $[KMnO_4]_o = 4.00 \times 10^{-4}$ M, [L-phenylalanine] = 5.00×10^{-3} M, $[KH_2PO_4] = 4.80 \times 10^{-2}$ M -0.144 M, $[K_2HPO_4]$ = 0.120-0.240 M, I = 0.504-0.768 M.

pH	k_1 / 10^{-5} s^{-1}	k_2 / 10^{-4} s^{-1}	k_3 / M^{-1} s^{-1}
6.655 ± 0.009	2.22 ± 0.05	3.31 ± 0.23	0.222 ± 0.002
6.826 ± 0.004	3.27 ± 0.05	4.77 ± 0.18	0.329 ± 0.010
7.021 ± 0.004	4.81 ± 0.10	4.77 ± 0.86	0.501 ± 0.025
7.229 ± 0.006	6.04 ± 0.13	9.93 ± 1.03	0.565 ± 0.017
7.471 ± 0.007	8.24 ± 0.20	25.91 ± 2.49	0.691 ± 0.002

(a) Errors associated to the pH values are standard deviations (10 determinations).
(b) Errors associated to the pseudo-rate constants were calculated as a half of the range (2 determinations).

Table 6. Values of the pseudo-rate constants at 25.0 ºC and different pHs. $[KMnO_4]_o = 4.00 \times 10^{-4}$ M, [L-phenylalanine] = 5.00×10^{-3} M, $[KH_2PO_4] = 4.80 \times 10^{-2}$ M -0.144 M, $[K_2HPO_4]$ = 0.120-0.240 M, I = 0.504-0.768 M.

pH	k_1 / 10^{-5} s^{-1}	k_2 / 10^{-4} s^{-1}	k_3 / M^{-1} s^{-1}
6.655 ± 0.009	3.47 ± 0.15	5.72 ± 0.94	0.368 ± 0.022
6.826 ± 0.004	5.23 ± 0.03	6.43 ± 0.07	0.601 ± 0.008
7.021 ± 0.004	7.90 ± 0.01	6.68 ± 0.23	0.866 ± 0.014
7.229 ± 0.006	9.53 ± 0.03	16.08 ± 1.80	0.935 ± 0.036
7.471 ± 0.007	13.60 ± 0.10	34.28 ± 1.93	1.172 ± 0.018

(a) Errors associated to the pH values are standard deviations (10 determinations).
(b) Errors associated to the pseudo-rate constants were calculated as a half of the range (2 determinations).

Table 7. Values of the pseudo-rate constants at 30.0 ºC and different pHs. $[KMnO_4]_0 = 4.00 \times 10^{-4}$ M, [L-phenylalanine] = 5.00×10^{-3} M, $[KH_2PO_4] = 4.80 \times 10^{-2}$ M -0.144 M, $[K_2HPO_4]$ = 0.120-0.240 M, *I* = 0.504-0.768 M.

pH	k_1 / 10^{-5} s^{-1}	k_2 / 10^{-4} s^{-1}	k_3 / M^{-1} s^{-1}
6.655 ± 0.009	5.69 ± 0.09	6.47 ± 0.98	0.661 ± 0.041
6.826 ± 0.004	8.18 ± 0.22	9.42 ± 0.58	0.985 ± 0.023
7.021 ± 0.004	11.51 ± 0.75	14.12 ± 1.01	1.193 ± 0.027
7.229 ± 0.006	15.09 ± 0.18	31.83 ± 2.40	1.415 ± 0.016
7.471 ± 0.007	20.78 ± 0.03	89.29 ± 1.14	1.871 ± 0.027

(a) Errors associated to the pH values are standard deviations (10 determinations).
(b) Errors associated to the pseudo-rate constants were calculated as a half of the range (2 determinations).

Table 8. Values of the pseudo-rate constants at 35.0 ºC and different pHs. $[KMnO_4]_0 = 4.00 \times 10^{-4}$ M, [L-phenylalanine] = 5.00×10^{-3} M, $[KH_2PO_4] = 4.80 \times 10^{-2}$ M -0.144 M, $[K_2HPO_4]$ = 0.120-0.240 M, *I* = 0.504-0.768 M.

pH	k_1 / 10^{-5} s^{-1}	k_2 / 10^{-4} s^{-1}	k_3 / M^{-1} s^{-1}
6.655 ± 0.009	8.55 ± 0.03	9.60 ± 0.11	1.121 ± 0.012
6.826 ± 0.004	13.18 ± 0.05	13.95 ± 0.36	1.579 ± 0.046
7.021 ± 0.004	17.00 ± 0.06	25.63 ± 1.79	1.864 ± 0.042
7.229 ± 0.006	23.65 ± 0.15	48.12 ± 1.64	2.399 ± 0.033
7.471 ± 0.007	30.52 ± 0.52	165.47 ± 15.51	3.003 ± 0.005

(a) Errors associated to the pH values are standard deviations (10 determinations).
(b) Errors associated to the pseudo-rate constants were calculated as a half of the range (2 determinations).

Table 9. Values of the pseudo-rate constants at 40.0 ºC and different pHs. $[KMnO_4]_o = 4.00 \times 10^{-4}$ M, [L-phenylalanine] = 5.00×10^{-3} M, $[KH_2PO_4] = 4.80 \times 10^{-2}$ M -0.144 M, $[K_2HPO_4]$ = 0.120-0.240 M, I = 0.504-0.768 M.

13.5. EFFECT OF TEMPERATURE

The activation parameters obtained from the pseudo-rate constants at different pHs (Tables 5-9) by application of the Arrhenius (activation energy) and Eyring (standard activation enthalpy and entropy) equations are given in Tables 10-12.

pH	E_a / kJ mol^{-1}	$\Delta H^{\circ}_{\neq}$ / kJ mol^{-1}	$\Delta S^{\circ}_{\neq}$ / J K^{-1} mol^{-1}
6.655 ± 0.009	68.7 ± 1.3	66.2 ± 1.3	-67.7 ± 4.3
6.826 ± 0.004	70.9 ± 0.8	68.4 ± 0.8	-57.2 ± 2.6
7.021 ± 0.004	65.9 ± 1.5	63.4 ± 1.5	-70.8 ± 5.1
7.229 ± 0.006	70.1 ± 0.5	67.6 ± 0.5	-54.9 ± 1.5
7.471 ± 0.007	67.8 ± 1.3	65.3 ± 1.3	-59.8 ± 4.2

(a) Errors associated to the pH values are standard deviations (10 determinations).
(b) Errors associated to activation parameters were calculated from the standard deviations for the intercept and slope of the Arrhenius and Eyring plots.

Table 10. Values of the apparent activation parameters associated to the pseudo-rate constant k_1 at different pHs. $[KMnO_4]_o = 4.00 \times 10^{-4}$ M, [L-phenylalanine] = 5.00×10^{-3} M, $[KH_2PO_4] = 4.80 \times 10^{-2}$ M -0.144 M, $[K_2HPO_4]$ = 0.120-0.240 M, I = 0.504-0.768 M, 20.0-40.0 ºC.

pH	E_a / kJ mol^{-1}	$\Delta H^{\circ}_{\neq}$ / kJ mol^{-1}	$\Delta S^{\circ}_{\neq}$ / J K^{-1} mol^{-1}
6.655 ± 0.009	53.5 ± 4.8	51.0 ± 4.8	-140.1 ± 15.9
6.826 ± 0.004	56.0 ± 1.7	53.5 ± 1.7	-129.4 ± 5.6
7.021 ± 0.004	81.9 ± 7.0	79.4 ± 7.0	-42.4 ± 23.1
7.229 ± 0.006	81.5 ± 3.3	79.0 ± 3.3	-37.3 ± 10.9
7.471 ± 0.007	106.3 ± 8.8	103.8 ± 8.8	52.0 ± 29.0

(a) Errors associated to the pH values are standard deviations (10 determinations).
(b) Errors associated to activation parameters were calculated from the standard deviations for the intercept and slope of the Arrhenius and Eyring plots.

Table 11. Values of the apparent activation parameters associated to the pseudo-rate constant k_2 at different pHs. $[KMnO_4]_0 = 4.00 \times 10^{-4}$ M, [L-phenylalanine] = 5.00×10^{-3} M, $[KH_2PO_4] = 4.80 \times 10^{-2}$ M - 0.144 M, $[K_2HPO_4]$ = 0.120-0.240 M, I = 0.504-0.768 M, 20.0-40.0 ºC.

pH	E_a / kJ mol^{-1}	$\Delta H^{\circ}_{\neq}$ / kJ mol^{-1}	$\Delta S^{\circ}_{\neq}$ / J K^{-1} mol^{-1}
6.655 ± 0.009	83.6 ± 1.3	81.1 ± 1.3	58.5 ± 4.2
6.826 ± 0.004	78.0 ± 2.1	75.5 ± 2.1	43.7 ± 6.9
7.021 ± 0.004	68.7 ± 2.8	66.2 ± 2.8	15.3 ± 9.2
7.229 ± 0.006	73.5 ± 1.5	71.0 ± 1.5	32.4 ± 4.9
7.471 ± 0.007	73.8 ± 1.2	71.2 ± 1.2	35.3 ± 4.0

(a) Errors associated to the pH values are standard deviations (10 determinations).
(b) Errors associated to activation parameters were calculated from the standard deviations for the intercept and slope of the Arrhenius and Eyring plots.

Table 12. Values of the apparent activation parameters associated to the pseudo-rate constant k_3 at different pHs. $[KMnO_4]_0 = 4.00 \times 10^{-4}$ M, [L-phenylalanine] = 5.00×10^{-3} M, $[KH_2PO_4] = 4.80 \times 10^{-2}$ M - 0.144 M, $[K_2HPO_4]$ = 0.120-0.240 M, I = 0.504-0.768 M, 20.0-40.0 ºC.

Both the activation energy and enthalpy associated to rate constant k_1 were independent of the pH, whereas those associated to k_2 increased with increasing pH and those associated to k_3 decreased. With respect to the activation entropy, those associated to both k_1 and k_2 increased with increasing pH, whereas that associated to k_3 decreased.

14. MECHANISM

According to the information reported in the literature concerning the reaction products,[71] the stoichiometries of the permanganate oxidation of α-amino acids to yield Mn(IV) and Mn(III) can be written, respectively, as:

$$2MnO_4^- + 3NH_3^+CHRCO_2^- + 5H^+ = 2MnO_2 + 3NH_4^+ + 3RCHO + 3CO_2 + H_2O \quad (37)$$

$$2MnO_4^- + 4NH_3^+CHRCO_2^- + 6H^+ = Mn_2O_3 + 4NH_4^+ + 4RCHO + 4CO_2 + H_2O \quad (38)$$

where in the case of the present study R = $C_6H_5CH_2$ (phenylmethyl).

Based on the experimental results found both in the present study and in others[72,73] previously reported, the following mechanism can be proposed for the non-autocatalytic part of the reaction:

$$^+H_3NCHRCO_2^- \underset{}{\overset{K_I}{\rightleftharpoons}} H_2NCHRCO_2^- + H^+ \quad (39)$$

$$MnO_4^- + {}^+H_3NCHRCO_2^- \xrightarrow[\text{slow}]{k_{II}} HMnO_4^- + H_2NC^{\cdot}RCO_2^- + H^+ \quad (40)$$

$$MnO_4^- + H_2NCHRCO_2^- \xrightarrow[\text{slow}]{k_{III}} HMnO_4^- + H_2NC^{\cdot}RCO_2^- \quad (41)$$

$$H_2NC^{\cdot}RCO_2^- + H_2O \longrightarrow H_2NC^{\cdot}HR + CO_2 + HO^- \quad (42)$$

$$MnO_4^- + H_2NC^{\cdot}HR \longrightarrow HMnO_4^- + HN{=}CHR \quad (43)$$

$$HN{=}CHR + H_3O^+ \longrightarrow NH_4^+ + RCHO \quad (44)$$

$$HMnO_4^- \rightleftharpoons MnO_4^{2-} + H^+ \quad (45)$$

$$HMnO_4^- + MnO_4^{2-} \longrightarrow HMnO_4^{2-} + MnO_4^- \quad (46)$$

$$HMnO_4^{2-} + H_2NCHRCO_2^- \longrightarrow MnO_2 + H_2NC^{\cdot}RCO_2^- + 2HO^- \quad (47)$$

$$nMnO_2 \longrightarrow (MnO_2)_n \quad (48)$$

On the other hand, the mechanism that can be proposed for the autocatalytic part of the reaction consists of these elementary steps:

$$(MnO_2)_n + {}^+H_3NCHRCO_2^- \overset{K_{IV}}{\rightleftharpoons} (MnO_2)_n - {}^+H_3NCHRCO_2^- \quad (49)$$

$$(MnO_2)_n - {}^+H_3NCHRCO_2^- \overset{K_V}{\rightleftharpoons} (MnO_2)_n - H_2NCHRCO_2^- + H^+ \quad (50)$$

$$(MnO_2)_n - {}^+H_3NCHRCO_2^- \xrightarrow[\text{slow}]{k_{VI}} (MnO_2)_{n-1} - MnO + HN{=}CHR + CO_2 + H_2O \quad (51)$$

$$(MnO_2)_n - H_2NCHRCO_2^- \xrightarrow[\text{slow}]{k_{VII}} (MnO_2)_{n-1} - MnO + HN{=}CHR + CO_2 + HO^- \quad (52)$$

$$(MnO_2)_{n-1} - MnO + {}^+H_3NCHRCO_2^- \overset{K_{VIII}}{\rightleftharpoons} (MnO_2)_{n-1} - MnO - {}^+H_3NCHRCO_2^- \quad (53)$$

$$(MnO_2)_{n-1} - MnO - {}^+H_3NCHRCO_2^- \overset{K_{IX}}{\rightleftharpoons} (MnO_2)_{n-1} - MnO - H_2NCHRCO_2^- + H^+ \quad (54)$$

$$MnO_4^- + (MnO_2)_{n-1} - MnO - {}^+H_3NCHRCO_2^- \xrightarrow[\text{slow}]{k_X} (MnO_2)_{n+1} + H_2NC^{\cdot}RCO_2^- + H_2O \quad (55)$$

$$MnO_4^- + (MnO_2)_{n-1} - MnO - H_2NCHRCO_2^- \xrightarrow[\text{slow}]{k_{XI}} (MnO_2)_{n+1} + H_2NC^{\cdot}RCO_2^- + HO^- \quad (56)$$

$$(MnO_2)_{n-1} - MnO \longrightarrow (MnO_2)_{n-2} - Mn_2O_3 \quad (57)$$

In the proposed mechanism four reaction pathways can be differentiated, each explaining the global stoichiometry: (i) non-autocatalytic pathway without acid-base catalysis, (ii) non-autocatalytic pathway with base catalysis, (iii) autocatalytic pathway without acid-base catalysis and (iv) autocatalytic pathway with base catalysis. One rate-determining (slow) step has been proposed for each of the two non-autocatalytic pathways, corresponding to the experimental rate constant k_1. For each autocatalytic pathway, two rate-determining steps have been proposed because of the involvement of a long-lived intermediate, $(MnO_2)_{n-1} - MnO$, too stable to be in steady state. This intermediate divides each autocatalytic reaction pathway in two parts, corresponding to two different experimental rate constants (k_2 and k_3). In every case the proposed slow step is coincident with the first redox elementary reaction.

By application of the quasi-equilibrium approximation to the fast reversible reactions placed in the mechanism before the rate-determining steps (eqs 39, 49, 50, 53 and 54) and of the steady-state approximation to the short-lived intermediates [all but $(MnO_2)_{n-1} - MnO$], the following mathematical expressions can be inferred for the three experimental rate constants:

$$k_1 = \frac{(k_{II}\,[H^+] + K_I\,k_{III})\,[\text{L-Phe}]_T}{2\,(K_I + [H^+])} \quad (58)$$

$$k_2 = \frac{K_{IV}\,(k_{VI}\,[H^+] + K_V\,k_{VII})\,[\text{L-Phe}]_T}{(1 + K_{IV}\,[\text{L-Phe}]_T)\,(K_V + [H^+])} \quad (59)$$

$$k_3 = \frac{K_{VIII}\,(k_X\,[H^+] + K_{IX}\,k_{XI})\,[\text{L-Phe}]_T}{K_{IX} + [H^+]} \quad (60)$$

where $[\text{L-Phe}]_T$ is the total amino acid concentration (both the zwitterionic and anionic forms included). The value of the equilibrium constant associated to eq 39 has been reported (K_I = 5.16×10^{-10} M, pK_a = 9.29, at zero ionic strength).[74]

Equations 58 and 60 are consistent with the increase of rate constants k_1 and k_3 with increasing amino acid concentration. Equation 59 is consistent with the independence of rate constant k_2 of the amino acid concentration provided that $K_{IV}\,[\text{L-Phe}]_T >> 1$. This condition would correspond to saturation of the colloid surface by the amino acid. Actually, kinetic laws of zero order in the substrate are very frequent in surface reactions.[75] The increase of the experimental rate constant k_1 with increasing ionic strength is consistent with the fact that the theoretical rate constant k_{III} corresponds to the elementary reaction of two anions (eq 41), since the presence of inert ions (K^+ and Cl^-) in the solution weakens the electrostatic repulsion between the two reactants (permanganate ion and the anionic form of the amino acid), thus increasing the frequency of their collisions. Finally, eqs 58-60 are also consistent with the increase of the three experimental rate constants with increasing pH provided that $k_{III} > k_{II}$, $k_{VII} > k_{VI}$ and $k_{XI} > k_X$. These conditions are indeed plausible because the anionic form of the amino acid has a higher electronic density (and so a higher reducing power) than the zwitterionic form.

15. CONCLUSIONS

(i) Permanganate ion is reduced by L-phenylalanine in aqueous phosphate-buffered neutral media to a mixture of colloidal manganese(IV) and manganese(III) oxides ($MnO_2 - Mn_2O_3$).

(ii) The colloidal particles formed as reaction products do not precipitate during the course of the reaction because of their mutual electrostatic repulsion due to the adsorption of phosphate ions on the colloid surface.

(iii) The decay of permanganate ion and the formation of the $MnO_2 - Mn_2O_3$ colloidal product can be followed spectrophotometrically at 525 and 420 nm, respectively.

(iv) The permanganate oxidation of L-phenylalanine is autocatalyzed by its colloidal reaction product.

(v) A BASIC-language program allows the determination of three experimental rate constants (k_1, k_2 and k_3) for each kinetic experiment. Rate constant k_1 corresponds to the permanganate-amino acid reaction in the solution, k_2 to the reduction of Mn(IV) to Mn(II), and k_3 to the re-oxidation of Mn(II) by Mn(VII).

(vi) Rate constants k_1 and k_3 increase with increasing amino acid concentration, whereas k_2 shows no appreciable dependence on that variable.

(vii) Addition of potassium chloride to the reaction media leads to an increase of rate constant k_1 and a decrease of k_2, k_3 remaining almost constant.

(viii) The three rate constants increase with increasing pH in the range 6.65-7.47 (base catalysis).

(ix) An increase in the pH leads to an increase of the activation energy associated to rate constant k_2 and a decrease of the activation energy associated to k_3, whereas that associated to k_1 shows no appreciable variation.

(x) A reaction mechanism involving $(MnO_2)_{n-1} - MnO$ as a long-lived intermediate and all the other intermediates in steady state, consistent with the experimental information available on rate constants k_1, k_2 and k_3, has been proposed.

16. REFERENCES

1. Freeman, F. Postulated Intermediates and Activated Complexes in the Permanganate Ion Oxidation of Organic Compounds. *Rev. React. Species Chem. React.* **1976,** *1*, 179-226
2. Fatiadi, A. J. The Classical Permanganate Ion - Still a Novel Oxidant in Organic-Chemistry. *Synthesis.* **1987,** 85-127.
3. Singh, N.; Lee, D. G. Permanganate: A Green and Versatile Industrial Oxidant. *Org. Process Res. Dev.* **2001,** *5*, 599-603.
4. Kint, C.; Verstraeten, N.; Hofkens, J.; Fauvart, M.; Michiels, J. Bacterial Obg Proteins: GTPases at the Nexus of Protein and DNA Synthesis. *Crit. Rev. Microbiol.* **2014,** *40*, 207-224.
5. Wolff, S. P.; Garner, A.; Dean, R. T. Free Radicals, Lipids and Protein Degradation. *Trends Biochem. Sci.* **1986,** *11*, 27-31.
6. Ameta, S. C.; Pande, P. N.; Gupta, H. L.; Chowdhry, H. C. Kinetics of Oxidative Decarboxylation of L-Serine by Potassium Permanganate. *Acta Phys. Chem.* **1980,** *26*, 89-92.
7. Ameta, S. C.; Gupta, H. L.; Pande, P. N.; Chaudhary, H. C. Kinetics of Oxidative Decarboxylation of DL-Aspartic Acid by Potassium Permanganate. *Z. Phys. Chem. Leipzig* **1980,** *261*, 802-804.
8. Ameta, S. C.; Pande, P. N.; Gupta, H. L.; Chowdhry, H. C. Kinetic-Study of Oxidative Decarboxylation of L-Beta-Phenylalanine by Potassium-Permanganate. *Z. Phys. Chem. Leipzig* **1980,** *261*, 1222-1224.
9. Ameta, S. C.; Pande, P. N.; Gupta, H. L.; Chowdhry, H. C. Kinetics of Oxidative Decarboxylation of L-Cysteine by Permanganate. *Acta Chim. Academ. Sci. Hung.* **1982,** *110*, 7-11.
10. Hassan, R. M.; Mousa, M. A.; Wahdan, M. H. Kinetics and Mechanism of Oxidation of Beta-Phenylalanine by Permanganate Ion in Aqueous Perchloric-Acid. *J. Chem. Soc., Dalton Trans.* **1988,** 605-609.
11. Andres-Ordax, F. J.; Arrizabalaga, A.; Peche, R.; Quintana, M. A. Kinetic Study of Autocatalytic Oxidation of L Alanine by Potassium Permanganate in Acidic Medium pH 1-3. *An. Quim.* **1991,** *87,* 828-832.
12. Andres-Ordax, F. J.; Arrizabalaga, A.; Casado, J.; Peche, R. Kinetic Study of the Oxidation of L-Threonine by MnO4- Ions. *React. Kinet. Catal. Lett.* **1991,** *44,* 293-301.
13. Hassan, R. M. Kinetics and Mechanism of Oxidation of DL-Alpha-Alanine by Permanganate Ion in Acid Perchlorate Media. *Can. J. Chem.* **1991,** *69*, 2018-2023.
14. Andres-Ordax, F. J.; Arrizabalaga, A.; Casado, J.; Peche, R.; Quintana, M. A. Kinetic Study of the Autocatalytic Oxidation of Glicine by the Permanganate Ions in Acid-Medium (pH 1-3). *An. Quim.* **1992,** *88,* 440-443.
15. Insausti, M. J.; Mata-Perez, F.; Alvarez-Macho, M. P. Permanganate Oxidation of L-Alanine in Acidic Solvent-Autocatalysis by Intermediate Mn(IV) Species. *Collect. Czech. Chem. Commun.* **1994,** *59,* 528-538.
16. Insausti, M. J.; Mata-Perez, F.; Alvarez-Macho, M. P. Kinetic-Study of the Oxidation of L-Phenylalanine by Potassium-Permanganate in Acid-Medium. *Int. J. Chem. Kinet.* **1995,** *27,* 507-515
17. Insausti, M. J.; Mata-Perez, F.; Alvarez-Macho, M. P. Kinetic Study of the Oxidation of Glycine by Permanganate Ions in Acid Medium. *Collect. Czech. Chem. Commun.* **1996,** *61,* 232-241.
18. Arrizabalaga, A.; Andres-Ordax, F. J.; Fernandez-Aranguiz, M. Y.; Peche, R. Kinetics and Mechanism of the oxidation of L-Alpha-Amino-n-Butyric Acid by Permanganate in Acid Medium. *Int. J. Chem. Kinet.* **1996,** *28,* 799-805.

19. Iloukhani, H.; Bahrami, H. Kinetic Studies and Mechanism on the Permanganic Oxidation of L-Glutamine in Strong Acid Medium in the Presence and Absence of Silver(I). *Int. J. Chem. Kinet.* **1999,** *31,* 95-102.
20. Iloukhani, H.; Moazenzadeh, M. Thermodynamic and Kinetic Studies of Oxidation of L-Histidine by Manganese (VII) in Concentrated Sulfuric Acid Medium in the Absence and Presence of Silver(I). *Phys. Chem. Liq.* **2001,** *39,* 429-442.
21. Khan, F. H.; Ahmad, F. Micellar Effect on Two-Phase Kinetics of Oxidative Degradation of Lysine. *Oxid. Commun.* **2004,** *27,* 869-885.
22. Bahrami, H.; Zahedi, M. Kinetics and Mechanism of the Oxidation of L-Alpha-Amino-n-Butyric Acid in Moderately Concentrated Sulfuric Acid Medium. *Can. J. Chem.* **2004,** *82,* 430-436.
23. Zahedi, M.; Bahrami, H. Kinetics and Mechanism of the Autocatalytic Oxidation of L-Asparagine in a Moderately Concentrated Sulfuric Acid Medium. *Kinet. Catal.* **2004,** *45,* 351-358.
24. Bahrami, H.; Zahedi, M. Delayed Autocatalytic Behavior of Mn(II) Ions at a Critical Ratio: The Effect of Structural Isomerism on Permanganic Oxidation of L-Norleucine. *Int. J. Chem. Kinet.* **2006,** *38,* 1-11.
25. Andres-Ordax, F. J.; Arrizabalaga, A.; Martinez, J. I. Kinetic-Study of the Oxidation of L-Phenylalanine by Potassium-Permanganate in Neutral Medium. *An. Quim.* **1984,** *80,* 531-535.
26. Garrido, J. A.; Perez-Benito, J. F.; Rodríguez, R. M.; De Andres, J.; Brillas, E. Auto-Catalysis by Colloidal Manganese-Dioxide in the Permanganate Oxidation of L-Isoleucine. *J. Chem. Res. (S)* **1987,** 380-381.
27. Brillas, E.; Garrido, J. A.; Perez-Benito, J. F.; Rodríguez, R. M.; De Andres, J. Kinetic Study of Permanganate Oxidation of L-Leucine in Neutral Aqueous-Solution. *Collect. Czech. Chem. Commun.* **1988,** *53,* 479-486.
28. De Andres, J.; Brillas, E.; Garrido, J. A.; Perez-Benito, J. F.; Rodríguez, R. M. The Reaction Between L-Glutamic Acid and Permanganate Ion in Neutral Aqueous-Solutions. *Gazz. Chim. Ital.* **1988,** *118,* 203-207.
29. De Andres, J.; Brillas, E.; Garrido, J. A.; Perez-Benito, J. F. Kinetics and Mechanisms of the Oxidation by Permanganate of L-Alanine. *J. Chem. Soc., Perkin Trans. 2.* **1988,** 107-112.
30. Rodríguez, R. M.; De Andres, J.; Brillas, E.; Garrido, J. A.; Perez-Benito, J. F. Autocatalytic Permanganate Oxidation of L-Threonine. *New. J. Chem.* **1988,** *12,* 143-146.
31. Andres-Ordax, F. J.; Arrizabalaga, A.; Ortega, K. Kinetic Chemical Studies in Autocatalytic Systems – Oxidations of L-Serine by Permanganate Ions. *An. Quim.* **1989,** *85,* 218-223.
32. Perez-Benito, J. F.; Rodríguez, R. M.; De Andres, J.; Brillas, E.; Garrido, J. A. Kinetics and Mechanisms of the Permanganate Oxidation of L-Valine in Neutral Aqueous-Solutions. *Int. J. Chem. Kinet.* **1989,** *21,* 71-81.
33. Insausti, M. J.; Mata-Perez, F.; Alvarez-Macho, M. P. Analysis of the Rate-Time Profits for the Permanganic Oxidation of Glycine. *An. Quim.* **1990,** *86,* 710-714.
34. Insausti, M. J.; Mata-Perez, F.; Alvarez-Macho, M. P. Permanganate Ion Oxidation of Glycine. *An. Quim.* **1991,** *87,* 821-827.
35. Insausti, M. J.; Mata-Perez, F.; Alvarez-Macho, M. P. Kinetic-Study of the Permanganate Oscidation of L-Alanine. *An. Quim.* **1991,** *87,* 877-883.
36. Insausti, M. J.; Mata-Perez, F.; Alvarez-Macho, M. P. Kinetics and Mechanisms of the Oxidation by Permanganate of L-Phenylalanine. *Int. J. Chem. Kinet.* **1991,** *23,* 593-605.
37. Insausti, M. J.; Mata-Perez, F.; Alvarez-Macho, M. P. Oxidation of Alpha-Amino-Acids by Permanganate – Isokinetic Relation. *Collect. Czech. Chem. Commun.* **1992,** *57,* 2331-2336.
38. Insausti, M. J.; Mata-Perez, F.; Alvarez-Macho, M. P. Permanganate Oxidation of Glycine – Influence of Amino-Acid on Colloidal Manganese-Dioxide. *Int. J. Chem. Kinet.* **1992,** *24,* 411-419.
39. Insausti, M. J.; Mata-Perez, F.; Alvarez-Macho, M. P. UV-Vis Spectrophotometric Study and Dynamic Analysis of the Colloidal Product of Permanganate Oxidation of Alpha-Amino-Acids. *Kinet. Catal. Lett.* **1993,** *51,* 51-59.

40. Andres-Ordax, F. J.; Aririzabalaga, A. Kinetic Treatment of Autocatalytic Reactions. *An. Quim.* **1985,** *81,* 431-852.
41. Mata, F.; Perez-Benito, J. F. The Kinetic Rate Law for Autocatalytic Reactions. *J. Chem. Educ.* **1987,** *64,* 925-927.
42. Perez-Benito, J. F.; Arias, C.; Brillas, E. Kinetic Treatment of Autocatalytic Reactions. *An. Quim.* **1991,** *87,* 849-852.
43. Perez-Benito, J. F. Permanganate Oxidation of a-Amino Acids: Kinetic Correlations for the Nonautocatalytic and Autocatalytic Reaction Pathways. *J. Phys. Chem.* **2011,** *115,* 9876-9885.
44. Perez-Benito, J. F. Autocatalytic Reaction Pathway on Manganese Dioxide Colloidal Particles in the Permanganate Oxidation of Glycine. *J. Phys. Chem.* **2009,** *113,* 15982-15991.
45. Wells, C. F.; Davies, G. A Spectrophotometric Investigation of the Aquomanganese(III) Ion in Perchlorate Media. *J. Chem. Soc. A* **1967,** 1858-1861.
46. Jaky, M.; Simandi, L. I. Mechanism of the Permanganate Oxidation of Unsaturated Compounds. Part I. Short-lived Intermediates of the Oxidation of Acetylenedicarboxylic Acid. *J. Chem. Soc., Perkin Trans. 2* **1972,** 1481-1486.
47. Adamcikova, L.; Krizova, A.; Valent, I. Kinetics of the Manganese(III)-Oxalate Reaction in Acidic Sulphate Media. *Transition Met. Chem.* **1993,** *18,* 218-220.
48. Perez-Benito, J. F.; Arias, C.; Amat, E. A Kinetic Study of the Reduction of Colloidal Manganese Dioxide by Oxalic Acid. *J. Colloid Interface Sci.* **1996,** *177,* 288-297.
49. Perez-Benito, J. F. Reduction of Colloidal Manganese Dioxide by Manganese(II). *J. Colloid Interface Sci.* **2002,** *248,* 130-135.
50. Barrow, G. M. *Physical Chemistry, 2nd ed.*; McGraw-Hill: New York, 1966, p 803.
51. Ogino, T.; Kikuiri, N. Evidence for the Existence of the Metastable Manganate(V). Ester Intermediate in the Permanganate Oxidation of *endo*-Dicyclopentadiene. *J. Am. Chem. Soc.* **1989,** *111,* 6174-6177.
52. Mata, F.; Perez-Benito, J. F. Mn(IV) Stabilized in Solution by Phosphate Ions. A Spectrophotometric Evidence of its Colloidal Nature. *Z. Phys. Chem. Leipzig.* **1986,** *267,* 120-124.
53. Mata-Perez, F.; Perez-Benito, J. F. Identification of the Product from the Reduction of Permanganate Ion by Trimethylamine in Aqueous Phosphate Buffers. *Can. J. Chem.* **1985,** *63,* 988-992.
54. Stewart, R. In *Oxidation in Organic Chemistry;* Wiberg, K. B.. Ed.; Academic Press: New York, 1965, p 8.
55. Taube, H. Catalysis of the Reaction of Chlorine and Oxalic Acid. Complexes of Trivalent Manganese in Solutions Containing Oxalic Acid. *J. Am. Chem. Soc.* **1947,** *69,* 1418-1428.
56. Taube, H. The Interaction of Manganic Ion and Oxalate. Rates, Equilibria and Mechanism. *J. Am. Chem. Soc.* **1948,** *70,* 1216-1220.
57. Pimienta, V.; Lavabre, D.; Levy, G.; Micheau, J. C. Comparative Behavior of the Autocatalytic $MnO_4^-/H_2C_2O_4$ Reaction in Open and Closed Systems. *J. Phys. Chem.* **1992,** *96,* 9298-9301.
58. Pimienta, V.; Lavabre, D.; Levy, G.; Micheau, J. C. Reactivity of the Mn(III) and Mn(IV) Intermediates in the Permanganate Oxalic-Acid Sulfuric-Acid Reaction-Kinetic Determination of the Reducing Species. *J. Phys. Chem.* **1994,** *98,* 13294-13299.
59. Pimienta, V.; Lavabre, D.; Levy, G.; Micheau, J. C. Kinetic Modeling of the $KMnO_4/H_2C_2O_4/H_2SO_4$ Reaction-Origin of the Bistability in a CSTR. *J. Phys. Chem.* **1995,** *99,* 14365-14371.
60. Wilkinson, F. *Chemical Kinetic and Reaction Mechanisms*; Van Nostrand Reinhold: New York, 1980, (a) p 72, (b) p 44.
61. Freeman, F.; Kappos, J. C. Permanganate Ion Oxidations. 15. Additional Evidence for Formation of Soluble (Colloidal) Manganese Dioxide during the Permanganate Ion Oxidation of Carbon-Carbon Double-Bonds in Phosphate-Buffered Solutions. *J. Am. Chem. Soc.* **1985,** *107,* 6628-6633.
62. Perez-Benito, J. F.; Lee, D. G. Oxidation of Hydrocarbons. 15. A Study of the Oxidation of Alkenes by Methyltributylammonium Permanganate. *Can. J. Chem.* **1985,** *63,* 3545-3550.
63. Perez-Benito, J. F.; Arias, C. Occurrence of Colloidal Manganese Dioxide in Permanganate Reactions. *J. Colloid Interface Sci.* **1992,** *152,* 70-84.

64. Mata, F.; Perez-Benito, J. F.; Arranz, A. A Kinetic Study of the Oxidation by Permanganate of Dimethylamine. *Z. Phys. Chem. Neue Folge.* **1983,** *135,* 141-156.
65. Mata, F.; Perez-Benito, J. F. Permanganate Ion Oxidation of Amines. Autocatalysis by Colloidal Manganese Dioxide. *Z. Phys. Chem. Neue Folge.* **1984,** *141,* 213-219.
66. Mata, F.; Perez-Benito, J. F. A Revision of the Kinetic Study of the Permanganate Ion Oxidation of Trimethylamine. *An. Quim.* **1985,** *81,* 79-81.
67. Mata, F.; Perez-Benito, J. F. An Analysis of the Activation Parameters in the Permanganate Ion Oxidation of Aliphatic Amines. *An. Quim.* **1987,** *83,* 459-466.
68. Mata, F.; Perez-Benito, J. F. Kinetics and Mechanisms of Oxidation of Methylamine by Permanganate Ion. *Can. J. Chem.* **1987,** *65,* 2373-2379.
69. Espenson, J. H. *Chemical Kinetics and Reaction Mechanisms*; McGraw-Hill: New York, 1995, p 112.
70. Perez-Benito, J. F; Mata, F.; Brillas, B. Permanganate Oxidation of Glycine: Kinetics, catalytic effects, and mechanisms. *Can. J. Chem.* **1987,** *65,* 2329-2337.
71. Zaheer, Z.; Rafiuddin. Sub- and Post-Micellar Catalytic and Inhibitory Effects of Cetyltrimethylammonium Bromide in the Permanganate Oxidation of Phenylalanine. *Colloids Surf. B Biointerfaces.* **2009,** *69,* 251-256.
72. Verma, R. S.; Reddy, M. J.; Shastry, V. R. Kinetic Study of Homogeneous Acid-Catalysed Oxidation of Certain Amino Acids by Potassium Permanganate in Moderately Concentrated Acidic Media. *J. Chem. Soc., Perkin Trans. 2.* **1976,** 469-473.
73. Panari, R. G.; Chougale, R. B.; Nandibewoor, S. T. Kinetics and Mechanism of Oxidation of L-Phenylalanine by Alkaline Permanganate. *Pol. J. Chem.* **1998,** *72,* 99-107.
74. Coetzee, J. F.; Ritchie, C. D. *Solute-Solvent Interactions*; Dekker: New York, 1969, p 17.
75. McCabe, R. W. Kinetics of Ammonia Decomposition on Nickel. *J. Catal.* **1983,** *79,* 445-450.

APPENDICES

APPENDIX 1: ABSORBANCE-TIME EXPERIMENTAL DATA FOR A TYPICAL KINETIC RUN

Time / min	*A*(420)	*A*(525)
0.3	0.011	0.895
4.3	0.012	0.889
8.3	0.015	0.882
12.3	0.016	0.875
16.3	0.018	0.869
20.3	0.019	0.862
24.3	0.021	0.857
28.3	0.022	0.856
32.3	0.023	0.850
36.3	0.025	0.844
40.3	0.027	0.838
44.3	0.028	0.832
48.3	0.031	0.825
52.3	0.032	0.819
56.3	0.034	0.813
60.3	0.035	0.807
64.3	0.038	0.800
68.3	0.040	0.794
72.3	0.042	0.787
76.3	0.043	0.780
80.3	0.045	0.773
84.3	0.047	0.767
88.3	0.049	0.760
92.3	0.051	0.753
96.3	0.053	0.746
100.3	0.055	0.739
104.3	0.057	0.732
108.3	0.060	0.725
112.3	0.062	0.717

116.3	0.062	0.712
120.3	0.065	0.704
124.3	0.067	0.697
128.3	0.069	0.690
132.3	0.072	0.682
136.3	0.074	0.675
140.3	0.076	0.668
144.3	0.078	0.661
148.3	0.079	0.653
152.3	0.082	0.646
156.3	0.084	0.638
160.3	0.087	0.631
164.3	0.089	0.623
168.3	0.091	0.616
172.3	0.093	0.608
176.3	0.094	0.600
180.3	0.097	0.593
184.3	0.099	0.586
188.3	0.101	0.578
192.3	0.104	0.570
196.3	0.106	0.563
200.3	0.108	0.556
204.3	0.111	0.548
208.3	0.112	0.541
212.3	0.114	0.534
216.3	0.116	0.526
220.3	0.117	0.518
224.3	0.120	0.510
228.3	0.122	0.503
232.3	0.124	0.496
236.3	0.127	0.489
240.3	0.128	0.482
244.3	0.131	0.475
248.3	0.133	0.469
252.3	0.135	0.461
256.3	0.138	0.455
260.3	0.139	0.448
264.3	0.140	0.441
268.3	0.143	0.434

272.3	0.145	0.427
276.3	0.147	0.421
280.3	0.149	0.414
284.3	0.151	0.407
288.3	0.152	0.401
292.3	0.154	0.393
296.3	0.156	0.388
300.3	0.157	0.381
304.3	0.159	0.375
308.3	0.161	0.369
312.3	0.163	0.363
316.3	0.164	0.357
320.3	0.166	0.351
324.3	0.168	0.345
328.3	0.169	0.339
332.2	0.171	0.334
336.3	0.173	0.327
340.3	0.174	0.323
344.3	0.176	0.317
348.3	0.177	0.312
352.3	0.178	0.308
356.3	0.180	0.302
360.3	0.182	0.296
364.3	0.183	0.291
368.3	0.184	0.286
372.3	0.186	0.281
376.3	0.187	0.276
380.3	0.188	0.272
384.3	0.189	0.268
388.3	0.190	0.264
392.3	0.192	0.259
396.3	0.193	0.254
400.3	0.195	0.250
404.3	0.195	0.246
408.3	0.197	0.242
412.3	0.198	0.238
416.3	0.199	0.235
420.3	0.200	0.230
424.3	0.200	0.227

428.3	0.202	0.223
432.3	0.203	0.219

Absorbances at 420 and 525 nm measured periodically at 4-min intervals during the course of a typical kinetic run. $[KMnO_4]_o = 4.00 \times 10^{-4}$ M, [L-phenylalanine] = 5.00×10^{-3} M, $[KH_2PO_4] = 0.120$ M, $[K_2HPO_4] = 0.150$ M, $I = 0.570$ M, pH 6.826 ± 0.004, 25.0 °C.